THEORETICAL STUDIES OF IMPORTANT PROCESSES IN PLANETARY AND COMET ATMOSPHERES

Renewal Request

April 21, 1989

NASA Grant NAGW 1404

Steven L. Guberman
Principal Investigator

Institute for Scientific Research
(Employer Identification # 22-248-7207)
33 Bedford St., Suite 19a
Lexington, MA 02173

The NASA Technical Officer for this Grant is

Dr. J. T. Bergstralh

Solar System Exploration Division, Code EL

NASA Headquarters, Washington, D. C. 20546

Principal Investigator

Steven L. Guberman
Physicist

617-861-7900

4/21/89

Institute Official

Susan L. Greenblatt
Grants Administrator

617-861-7900

4/21/89

This report is submitted to request the renewal of NASA Grant NAGW 1404 for the second year of funding, September 1, 1989-October 31, 1990.

I. Progress Report

Our current efforts have focused on the dissociative recombination (DR) of O_2^+, a process of great importance in planetary atmospheres. This process is difficult to study experimentally because of the need to determine the dependence of the product electronic states and kinetic energies upon the vibrational distribution of the ion and the electron temperature. The knowledge of these characteristics of DR is needed to accurately model planetary ionospheres. Using a theoretical quantum chemical approach, we have studied in detail the generation of $O(^1S)$ from DR,

$$O_2^+ + e^- \rightarrow O(^1S) + O(^1D), \qquad (1)$$

where e^- is an electron, both O atom products are excited, and the O_2^+ molecular ion may be vibrationally excited. Building upon earlier studies[1,2,3] which showed that (1) occurs along a $^1\Sigma_u^+$ molecular state, we have now included the indirect dissociative recombination mechanism. The latter process is similar to (1) except that instead of direct electron capture into a repulsive molecular state leading to dissociation to atoms, electron capture first occurs into an intermediate vibrationally excited Rydberg state followed by predissociation into atoms along the repulsive state used in the direct mechanism,

$$O_2^+ + e^- \rightarrow O_2(n,v) \rightarrow O(^1S) + O(^1D), \qquad (2)$$

where $O_2(n,v)$ is a neutral Rydberg state with principal quantum number n and vibrational level, v. These vibrationally excited Rydberg levels lie above the v=0 level of O_2^+ and are resonances in the electron-ion continuum. When the energy of the incoming electron coincides with the position of the Rydberg vibrational level a marked perturbation occurs in the DR cross section. We have found that the DR rate can also be altered by these Rydberg states.

The calculation of the full DR cross section including both the direct and indirect processes has required the calculation of the quantum defect of the $^1\Sigma_u^+$ Rydberg series and the autoionization width, both as a function of the internuclear distance. The cross sections have been calculated using molecular quantum defect theory.[4] Further details on these calculations are given in the first semi-annual progress report.

Figure 1 shows the cross sections for both the direct and indirect DR processes. The lower curve at low electron energies is relatively smooth across the range of electron energies plotted and corresponds to the direct DR cross section, i.e. there are no Rydberg excited vibrational levels included in the calculation. However, the direct DR curve has several abrupt decreases at 0.23eV, 0.46eV, 0.68eV, and 0.90eV. These energies correspond to the positions of the v=1,2,3 and 4 vibrational ion levels above the v=0 ion level. At each of these vibrational levels, a new channel for emitting the electron opens up and the DR cross section consequently drops. Some of these sudden decreases are partially obscured by the infinite series of resonances below each ion vibrational threshold which contribute to the

indirect DR process which is also plotted in the Figure. When the electron is emitted, the ion can be left in an excited vibrational level. The net result is electron impact vibrational excitation. Cross sections for the latter process have also been calculated and are discussed below.

The full cross section curve describing both the direct and indirect process is also shown in Figure 1. This curve has a very rich resonance structure giving rise to rapid variations in the cross section over narrow energy intervals. The full cross section curve is above the direct cross section curve even at low energies, where it is far from the first discernable resonance at 0.36eV. The source of the higher full cross section curve is the Rydberg level with principal quantum number n=6 and v=2. This level actually falls 0.0147eV below the v=0 level of the ion. However it is broadened by predissociation by the dissociating $^1\Sigma_u^+$ state. The broadening allows a wing of this resonance to appear above threshold. This resonance plays a large role in increasing the DR cross section at typical ionospheric temperatures (see below). The first resonance appears at 0.036eV and corresponds to the n=9 Rydberg $^1\Sigma_u^+$ state in the v=1 vibrational level. The resonance has a typical Beutler-Fano profile corresponding to a positive Fano q, i.e. the cross section first decreases and then increases as the energy is increased through the resonance position. The next resonance for n=10,v=1 appears at 0.076eV with a similar shape to that for n=9. As the electron energy approaches the v=1 ion level at 0.23eV, the infinite series of v=1 resonances interferes with resonances due to n=7,v=2 and n=4,v=6 at 0.12eV leading to a complex cross section shape in this region.

Figure 2 shows the DR rate constant for electron temperatures up to 3000K. The upper curve is from the full DR calculation and the lower curve

is for only direct DR in which the resonance states have been omitted. The full DR rate is 3.0 times larger that the direct DR rate at 300K and 2.6 times greater near 800K. The increase is primarily due to the n=6, v=2 resonance discussed above.

Figure 3 shows the calculated vibrational excitation cross section corresponding to the following process:

$$O_2^+(v=0) + e^- \rightarrow O_2^+(v=1) + e^-. \qquad (3)$$

The cross section for process (3) is calculated simultaneously with the calculation of the DR cross sections. Direct vibrational excitation by electron impact is often thought of as a slow process. However, its rate can be substantially increased if electronic resonance states can act as intermediate states. This is well known to be the case in the analogous excitation of neutral molecules where negative ion states play the intermediate role. There is very little in the literature on the excitation of molecular ions using neutral resonance states to assist the process. In the case of O_2^+, the cross section for excitation of the v=1 ion level has a sudden onset at the energy of the v=1 level, 0.23eV. Both the direct cross section, shown as the lower curve in Figure 3, and the full cross section, including both the direct and indirect processes, are shown. The direct cross section has abrupt breaks at the onset of higher excited vibrational levels. At the breaks, the cross section for v=1 excitation drops abruptly since a higher vibrational level can also be excited at these energies. At energies just below threshold, the cross section for the full DR process is considerably higher than that for direct DR and shows structure due to many

interfering resonance states.

The vibrational excitation rates are shown in Figure 4. The lower curve does not include the Rydberg resonances while the upper curve includes both direct and indirect DR. Clearly, the resonances play an important role in determining the magnitude of the excitation rate. The rate has a value of about 1.7×10^{-11} cm^3/sec at 800K. While this rate is not very large, it is important to remember that the repulsive $^1\Sigma_u^+$ state, which is studied here, does not cross the ion within the turning points of the v=1 vibrational level. However, there are other states which are known[2,3,5] to cross the ion within these turning points, e.g. $^3\Sigma_u^-$ and $^1\Delta_u$. These states could lead to high vibrational excitation for v=1. Studies of role of these states in vibrational excitation are currently in progress.

II. Plan of Work for 9/1/89-10/31/90

The plan of work for the next funding period will proceed in accord with the research discussed in the original proposal. The plan includes the completion of the ab initio calculation of the Rydberg and valence potential curves needed for the study of both direct and indirect DR leading to ^3P atoms. Only states having significant electron capture widths will be determined. These states will be used to calculate cross sections and rates for O_2^+ DR leading to ^3P atoms, using techniques developed during the first year of funding. The electronic widths of states leading to ^1D atoms will be calculated. For those states with large widths, the potential curves will also be determined. The important Rydberg states contributing to indirect recombination in the generation of ^1D atoms will be determined. DR cross

sections and rates for generating ^1D atoms will be calculated for both the direct and indirect processes. The results will yield a detailed picture of the DR of O_2^+ and will be invaluable for the modelling of the chemistry of planetary ionospheres. The kinetic energies and quantum yields of excited and ground state atoms will be determined as a function of electron temperature and ion vibrational excitation.

III. References

1. S. L. Guberman, Nature 327, 408 (1987).

2. S. L. Guberman, Planet. Space Sci. 36, 47 (1988).

3. S. L. Guberman, Ab Initio Studies of Dissociative Recombination, in Dissociative Recombination: Theory, Experiment, and Applications, ed. by J. B. A. Mitchell and S. L. Guberman (World Scientific, Singapore, 1989), p. 45.

4. A. Giusti, J. Phys. B 13, 3867 (1980).

5. S. L. Guberman, Potential Energy Curves for Dissociative Recombination, in Physics of Ion-Ion and Electron-Ion Collisions, ed. by F. Brouillard and J. W. McGowan (Plenum, New York, 1983) ,p.167

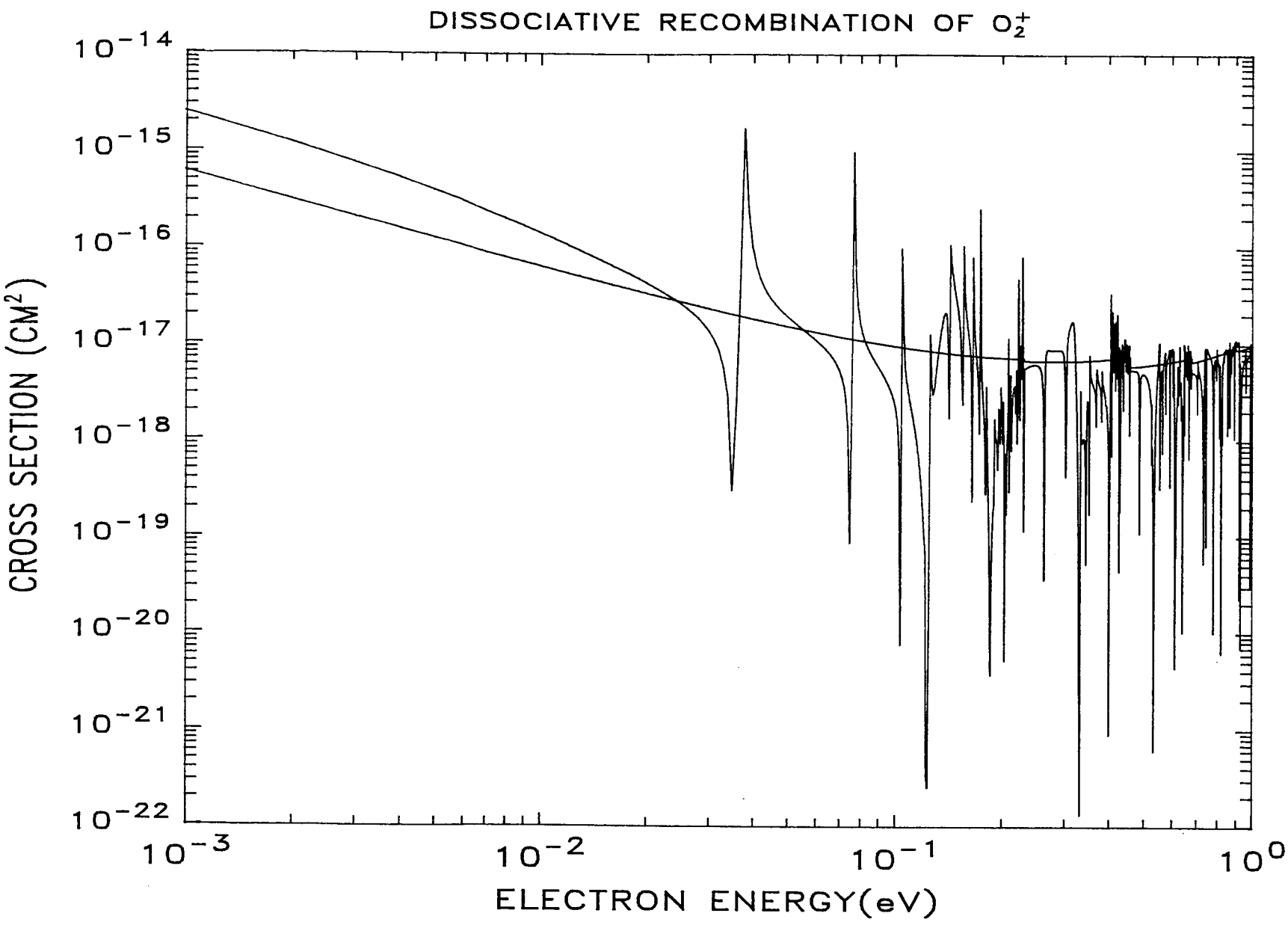
DISSOCIATIVE RECOMBINATION OF O_2^+
CROSS SECTION (CM^2)
10^{-14}
10^{-15}
10^{-16}
10^{-17}
10^{-18}
10^{-19}
10^{-20}
10^{-21}
10^{-22}
10^{-3}
10^{-2}
10^{-1}
10^{0}
ELECTRON ENERGY(eV)

Figure 1.

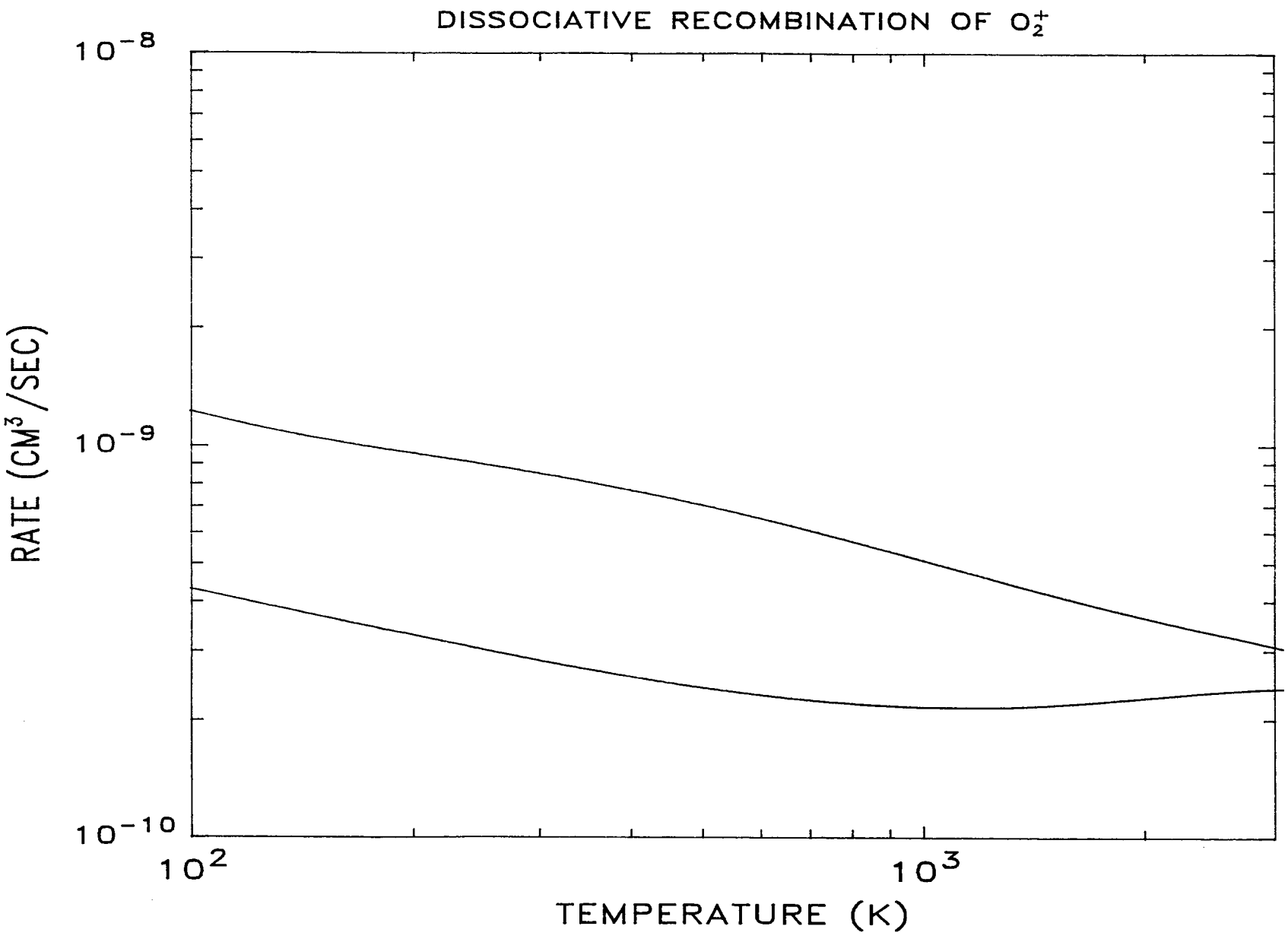
DISSOCIATIVE RECOMBINATION OF O_2^+
10^{-8}
10^{-9}
10^{-10}
RATE (CM^3/SEC)
10^2
10^3
TEMPERATURE (K)

Figure 2.

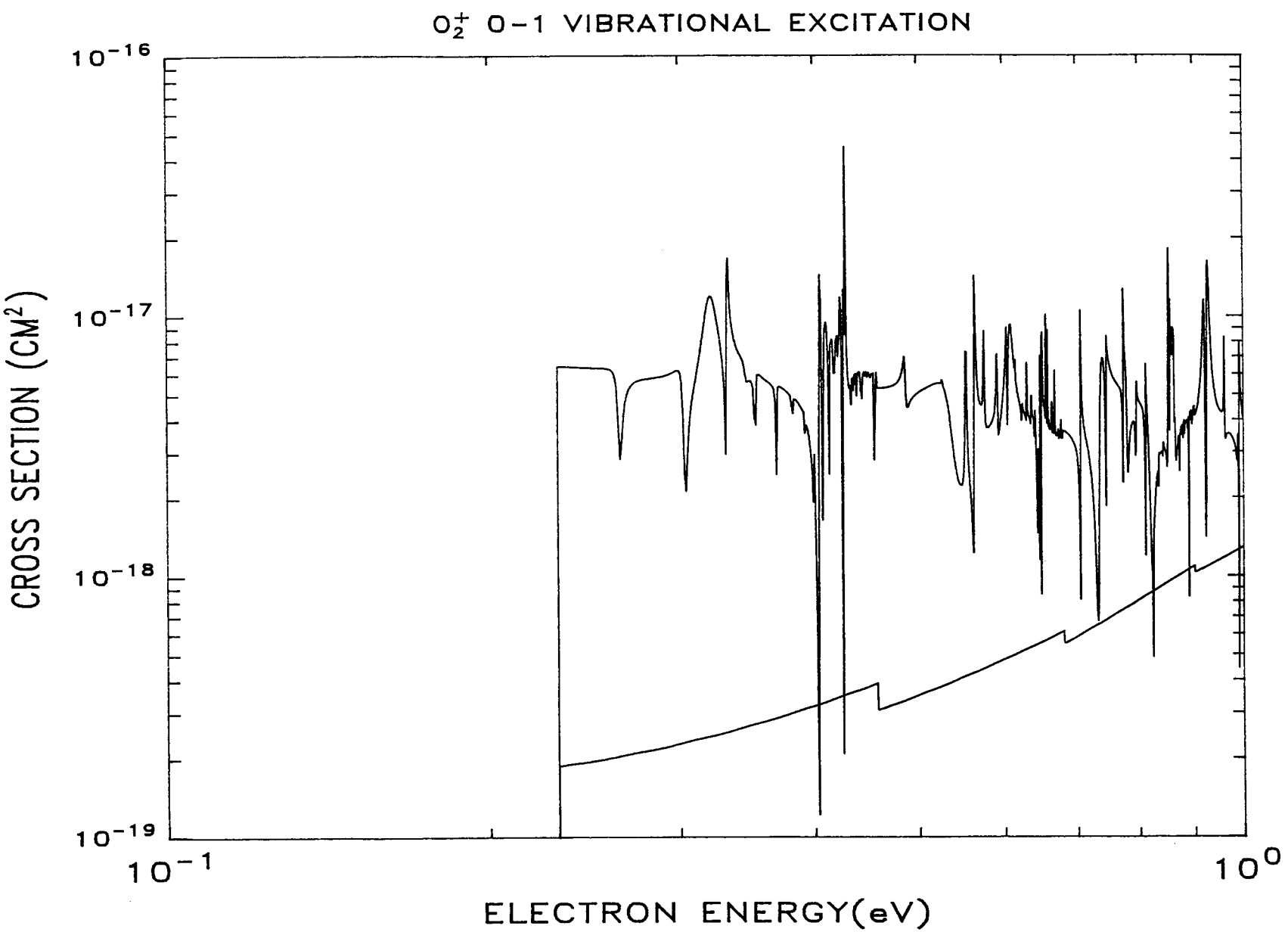
O_2^+ 0-1 VIBRATIONAL EXCITATION
CROSS SECTION (CM^2)
10^{-16}
10^{-17}
10^{-18}
10^{-19}
10^{-1}
10^{0}
ELECTRON ENERGY(eV)

Figure 3.

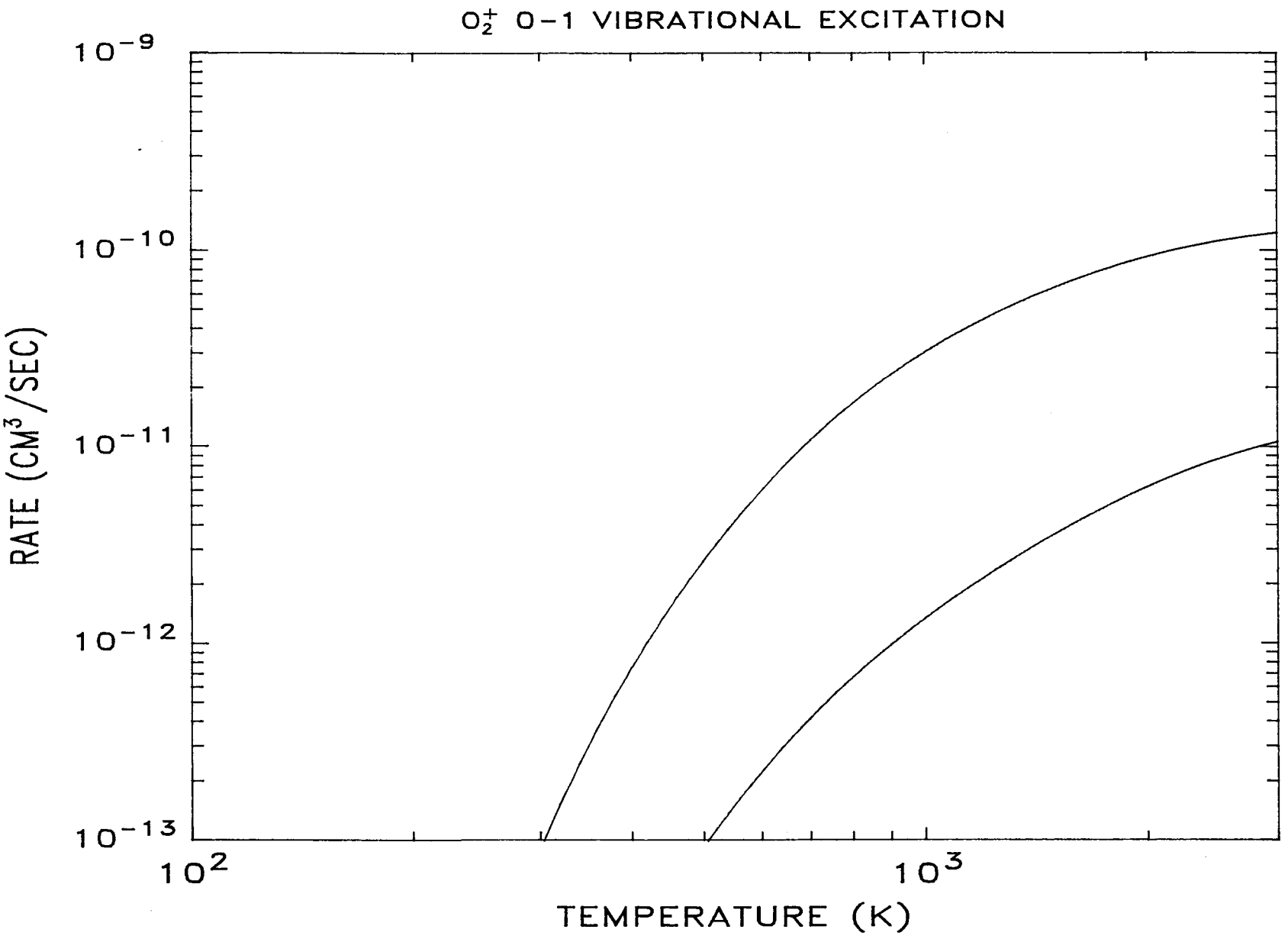
O_2^+ 0-1 VIBRATIONAL EXCITATION
10^{-9}
10^{-10}
10^{-11}
10^{-12}
10^{-13}
RATE (CM^3/SEC)
10^2
10^3
TEMPERATURE (K)

Figure 4.

IV. Budget for Year 2

September 1, 1989 - October 31, 1990

	Person months	Amount
Steven L. Guberman,P.I.	6	29,493
Fringe benefits		10,399
Phone		165
Supplies, postage, copying		260
Page charges		500
Travel		1,320
Secretarial Services		550
Total direct charges		42,687
Indirect cost @47.02%		20,071
Total		$62,758

V. Publications

1. S. L. Guberman, Ab Initio Studies of Dissociative Recombination, in Dissociative Recombination: Theory, Experiment, and Applications, ed. by J. B. A. Mitchell and S. L. Guberman (World Scientific, Singapore, 1989),p. 45.

2. S. L. Guberman and J. B. A. Mitchell, Introduction to Dissociative Recombination, in Dissociative Recombination: Theory, Experiment, and Applications, ed. by J. B. A. Mitchell and S. L. Guberman (World Scientific, Singapore, 1989),p.1.

3. K. Yoshino, A. S.-C. Cheung, J. R. Esmond, W. H. Parkinson, D. E. Freeman, S. L. Guberman, A. Jenouvrier, B. Coquart, and M. F. Merriemme, Improved Absorption Cross Section of Oxygen in the Wavelength Region 205-240nm of the Herzberg Continuum, Planet. Space Sci. 36, 1469 (1988).

4. J.-H. Yee, S. L. Guberman, and A. Dalgarno, Collisional Quenching of $O(^1D)$ by $O(^3P)$, to be submitted.

AB INITIO STUDIES OF DISSOCIATIVE RECOMBINATION

Steven L. Guberman
Institute for Scientific Research
33 Bedford St., Suite 19A
Lexington, MA 02173

ABSTRACT

Quantum chemical calculations of the dissociative recombination of O_2^+ and N_2^+ are reported. An approach for calculating autoionization widths from high principal quantum number Rydberg states is summarized and an example is presented for the lowest $^3\Pi_g$ dissociative state of O_2. For O_2^+, the $^1\Sigma_u^+$ state is the sole source of $O(^1S)$ from the lowest 10 vibrational levels of the ion. For $O(^1D)$, the $B^3\Sigma_u^-$, $^1\Sigma_u^+$, and $1^1\Delta_u$ states are the sources of $O(^1D)$ from the lowest three vibrational levels. Rate coefficients for generating $O(^1S)$ and $O(^1D)$ at ionospheric temperatures are reported. For N_2^+, states of $^3\Pi_u$, $^1\Sigma_g^+$ and $^3\Delta_g$ symmetries intersect the ion at the v=0 level. The configurational structure of these states indicates that the $^3\Pi_u$ states are likely to be the most important routes for dissociative recombination from v=0.

1. INTRODUCTION

Interest in dissociative recombination (DR) first arose out of the need to understand the properties of the Earth's ionosphere.[1],[2] Initial attention focused on the DR of O_2^+, N_2^+ and NO^+. While there has been much progress in the measurement of the total DR rate coefficients of these ions, the dependence of the quantum yield of excited and ground state atoms upon the electron temperature and ion vibrational level is only currently being unraveled. Impediments to experimental progress have included the difficulty of generating ions in specific vibrational levels and simultaneously identifying the atomic products.

Nevertheless there has been recent progress toward this goal.[3],[4],[5] An alternative theoretical approach based on spectroscopic identification of the potential curves which provide routes for DR is difficult since these states often do not have dipole allowed transitions from the ground state. Furthermore, electron capture occurs at high energies on the repulsive wall, well above the dissociation asymptote and out of range of the RKR approach. Additional difficulties include the paucity of information on electron capture widths although progress has been made in spectroscopic analysis of Rydberg-valence interactions[6],[7],[8],[9] from which widths can be derived.

Here, I review recent theoretical ab initio results obtained in this laboratory for the DR of O_2^+ and describe some preliminary results on the DR of N_2^+. For O_2^+, potential curves, electron capture widths and rate constants have been obtained for generating ^1S and ^1D atoms, the upper states of the green and red lines respectively. For N_2^+, potential curves for DR of the v=0 ion level have been computed.

2. WAVE FUNCTIONS

The wave functions calculated here are based on orbitals determined in either multiconfiguration or complete active space self consistent field (MCSCF or CASSCF) calculations. Each of the orbitals, ϕ_j, is expanded in a large set of Gaussian basis functions, χ_i,

$$\phi_j = \sum_i c_{j,i} \chi_i \qquad (1)$$

Some of the χ_i are individual Gaussian primitives[10] while others are fixed combinations (contractions) of Gaussian basis functions determined from atomic calculations.[11] The orbitals are used to construct large scale configuration interaction (CI) wave functions containing many configurations, each of which describes a possible distribution of the electrons in the molecular orbitals for a particular state symmetry. For example, for the $^1\Sigma_g^+$ ground state of N_2, the most important configuration near the equilibrium separation is:

$$(1\sigma_g)^2(1\sigma_u)^2(2\sigma_g)^2(2\sigma_u)^2(3\sigma_g)^2(1\pi_u)^4 \qquad (2)$$

The 1σ and 2σ orbitals are mostly N atom 1s and 2s orbitals, respectively. The $3\sigma_g$ orbital is a bonding combination consisting mostly of the N atom 2p orbitals lying along the bond axis. The $1\pi_u$ orbitals are out of plane bond orbitals consisting mostly of the N 2p orbitals that are perpendicular to the bond axis. Each configuration can have one or more spin couplings (referred to below as terms) for a given total spin symmetry. A wave function is constructed consisting of a superposition of many terms, Φ_i, each of which has the same total spin and spatial symmetry,

$$\psi_j = \sum_{i=1}^{N} C_{j,i}\ \Phi_i. \qquad (3)$$

In the CASSCF[12] approach a set of active orbitals is defined and N(CASSCF) terms are generated in (3) by taking all possible excitations of the electrons within this set while restricting each term to have the total spin and spatial symmetry of interest. Both the $c_{j,i}$ and the $C_{j,i}$ are determined by variationally optimizing the total energy of ψ_j. The MCSCF approach is identical except that usually a subset of the full active space is used. Since the orbitals are expanded in large basis sets, χ_i, the number of orbitals used in the CASSCF is only a subset of the orbitals that can be formed from the basis set. The CI wave functions are constructed by exciting electrons out of a small set of reference configurations into the remaining (virtual) orbitals. The reference configurations often consist of all the configurations needed to properly dissociate that particular state to the proper separated atoms limit. This approach leads to wave functions that are not biased to favor particular internuclear distances. Some of the wave functions reported here for N_2 include the 2σ orbitals in the active space and use the entire CASSCF wave function as a reference set. Taking at most one or two electrons from each of the reference configurations and promoting them to the virtual and other valence orbitals leads to a singles and doubles CI denoted CISD. The CI wave functions are expanded over the CASSCF orbitals and have the form of (3) with

N(CI)>>N(CASSCF). Some of calculations used here employ large scale wave functions having more than 100,000 terms with the CI coefficients determined by direct CI techniques.[13] Calculations have recently been completed on several states of N_2 and O_2 which provide examples of the sort of accuracy which can be expected with these techniques. For the ground state of N_2, 14 reference configurations (needed to properly dissociate the ground state to ^4S atoms) are used in the CI with a basis set consisting of 6s,3p,2d and 1f type contracted Gaussians leading to a CI wave function having 176,536 terms. The calculated (experimental[14]) spectroscopic constants are 2340.57(2356.56cm^{-1}) for ω_e, 14.27(14.3244cm^{-1}) for $\omega_e x_e$, and 2.0856(2.074347a_o) for the equilibrium distance, R_e. Similar calculations on the ground state of O_2 using a basis set of the same size leads to a 228,036 term wave function. The calculated (experimental[15]) results are 1565.47(1580.19) for ω_e, 10.93(11.98cm^{-1}) for $\omega_e x_e$, and 2.2999(2.2819a_o) for R_e. For O_2, a series of vertical excitation energies have been calculated. The calculated (experimentally derived) results are 5.8982(5.90±0.05eV) for $^1\Sigma_u^-$, 6.1318(6.11±0.05eV) for $^3\Delta_u$,6.2766(6.19±0.05eV) for $^3\Sigma_u^+$, and 8.66(8.61±0.05eV[16]) for $^3\Sigma_u^-$. All the experimental energies are derived from Ref.15 (except for $^3\Sigma_u^-$ by extending the RKR results with an ab initio repulsive wall.

Recent results have been obtained for N_2 using a [4s,3p,2d,1f] contracted Gaussian basis set and a CISD reference set consisting of the CASSCF configurations with 2σ in the active space. For the $C^3\Pi_u$ state the calculated (experimental)[14] results are 11.01(11.05eV) for T_e, 1986(2047cm^{-1}) for ω_e, 25.05(28.44cm^{-1}) for $\omega_e x_e$, and 2.1932(2.1707a_o) for R_e. For the $w^1\Delta_u$ state the results are 8.83(8.84eV) for T_e, 1532(1559cm^{-1}) for ω_e, 11.67(12.01cm^{-1}) for $\omega_e x_e$, and 2.4192(2.3977a_o) for R_e. The highly accurate values of the excitation energies and the other spectroscopic constants give us confidence that these repulsive curves will be located quite accurately relative to the ion potential curve.

3. POTENTIAL CURVES FOR O_2

Potential curves describing DR in O_2 and based on a [3s,2p,1d]

contracted Gaussian basis set and first order CI wave functions have been described previously.[17] These calculations showed that the $^1\Sigma_u^+$ state is the only state that can generate O(^{1}S) from the low vibrational levels. It crosses the ion between the outer turning points of the v=1 and v=2 vibrational levels and dissociates to the ^{1}D + ^{1}S asymptote. The next accessible state is $5^3\Pi_g$ which crosses the outer turning point of v=10. Among the states dissociating to O(^{1}S) there are three routes which cross the $a^4\Pi_u$ metastable state between the turning points for v=0. These routes with their dissociation limits shown in parentheses are $5^3\Pi_g(^3P + {}^1S)$, $5^3\Pi_u(^3P + {}^1S)$, and $4^1\Pi_g(^1D + {}^1S)$. Because of its spin symmetry, the $4^1\Pi_g$ state will have only a small DR rate coefficient from the metastable state. The remaining two states can lead to hot O atoms, each with 3.4eV kinetic energy. Future experiments designed to measure the ^{1}S quantum yield must be careful to be certain that no $a^4\Pi_u$ O_2^+ is generated which would interfere with the determination of the ^{1}S generated from the ion ground state.

For generating O(^{1}D), in addition to the $^1\Sigma_u^+$ state, the $B^3\Sigma_u^-$ state crosses the ion near the inner turning point of v=0 and leads to ^{3}P + ^{1}D atoms. A $^1\Delta_u$ state leading to two ^{1}D atoms crosses the ion near the outer turning point of v=0. The lowest valence state of $^1\Pi_g$ symmetry crosses the ion near the inner turning point of v=0 and can lead to ^{1}D atoms via a curve crossing with the $2^1\Pi_g$ state. At higher energies, the lowest $^3\Pi_g$ state crosses the ion near the inner turning point of the v=3 ion level and can lead to ^{1}D atoms via an avoided crossing with the $2^3\Pi_g$ state. The next accessible states for ^{1}D production are $2^3\Sigma_g^-(^1D + {}^3P)$, $2^3\Pi_g(^1D + {}^3P)$, and $2\ ^3\Pi_u(^1D + {}^3P)$ near the outer turning point of v=3, $3^3\Pi_g(^1D + {}^3P)$ and $2^1\Pi_g(^1D + {}^1D)$ near the outer turning point of v=4. As has been pointed out earlier[17], several of these routes are expected to have small electron capture widths.

The reader is referred to Ref. 17 for a discussion of additional routes that lead to only ground state atoms.

The important $B^3\Sigma_u^-$, $^1\Delta_u$, and $^1\Sigma_u^+$ states identified above have been the subject of larger scale calculations involving [6s,3p,2d,1f] contracted Gaussian basis sets and CI wave functions that include all single and double excitations to the virtual space.[18],[19] Second order

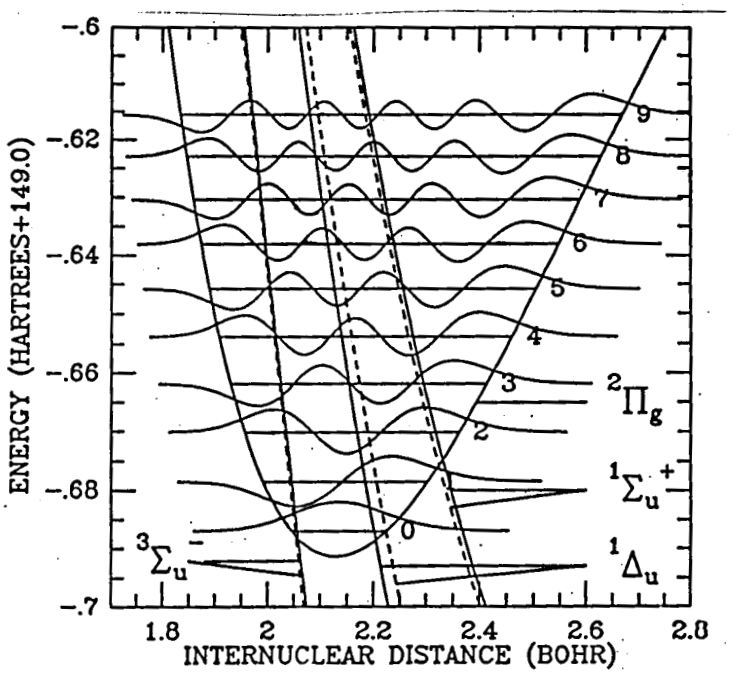

Fig. 1. Dissociative first order (dashed) and second order (solid) potentials for O_2 plotted with the ion potential from Ref. 15.

curves for the Π_g states have not been obtained because of their small widths (see below). Both the earlier curves and the large scale curves are plotted in Figure 1. The ion curve is the RKR[15] curve plotted at the experimental ionization potential above the large scale calculated ground state. The ion curve has been shifted to larger R to compensate for the difference between the calculated and experimental ground state R_e. In order to plot the first order curves on the same figure they have been shifted to larger R to correct for the difference between the first order and second order calculated R_e's. Also, the first order curves are shifted in energy so as to be plotted relative to the first order ground state. Relative to the ion, after the shift in the energy and distance coordinates, the curves are qualitatively similar. The largest difference is for $^1\Delta_u$ for which the second order curve is shifted by about $0.02a_o$ to smaller R near v=0 relative to the first order result.

4. ELECTRON CAPTURE WIDTHS FOR O_2

The DR cross section is approximately directly proportional to the

electron capture or autoionization width, Γ, a matrix element of the Hamiltonian operator, H, given by Fermi's golden rule:

$$\Gamma(R) = 2\pi\rho|\langle\Psi_f|H|\Psi_I^c\rangle|^2. \quad (4)$$

Ψ_I^c is the wave function of the properly antisymmetrized product of a "free" electron in a coulomb like orbital and the wave function for the ion. Ψ_f is the electronic wave function for the neutral state which describes the DR products and ρ is the density of states. Rydberg orbitals with high principal quantum numbers, n, have been used to describe the coulomb like orbital. Except for the Rydberg orbital, all the orbitals in (4) are bound and have large amplitude only near the molecule. As a result, it is only important to know the amplitude of the Rydberg orbital near the molecule. The inner part of coulomb orbitals are well known to be very similar to the inner part of high Rydberg orbitals.[20] With the coulomb orbital represented as a high Rydberg orbital all the orbitals in (4) are bound and are represented in terms of Gaussian basis functions.

For $n^*>>\ell$, where ℓ is the angular momentum quantum number, the matrix element in (4) can be closely represented by

$$|\langle\Psi_f|H|\Psi_I^c\rangle|^2 = (1/n^{*3})k\exp(-c/n^*) \quad (5)$$

where k and c are constants determined from the calculation of the matrix elements on the left side of (5) for the highest Rydberg states. These Rydberg states are nearly hydrogenic and the energies can be represented as $E=-(1/2(n^*)^2)$ where $n^*=n-\delta$ and δ is the quantum defect. The density of states can be written as

$$\rho = 1/(E(n^*-1/2) - E(n^*+1/2)) \quad (6)$$

which can be closely represented as

$$\rho = n^{*3}\exp(-1/(2n^{*2})). \quad (7)$$

Substituting (7) and (5) into (4) gives

$$\Gamma = 2\pi k \exp(-(c/n^*)-(.5/n^{*2})). \tag{8}$$

Taking the limit of $n^* \to \infty$ gives the threshold capture width,

$$\Gamma = 2\pi k. \tag{9}$$

The Rydberg wave functions have been refined further by optimizing them in the field of an optical potential due to the Ψ_f states. Feshbach projection operators[21] have been defined which partition the total space such that $\Psi = P\Psi + Q\Psi$ where $P\Psi$ contains the Rydberg states to be optimized and $Q\Psi$ are the Ψ_f states described above. In the usual Feshbach projection operator formalism, an eigenvalue equation is derived for $P\Psi$ that is difficult to solve because it contains an energy-dependent optical potential. However, using partitioning techniques,[22] $P\Psi$ can easily be determined by solving the usual CI problem. Writing the total wave function as $\Psi = P\Psi + Q\Psi$, we can write the Schroedinger equation in matrix form as

$$\begin{pmatrix} H_{PP} & H_{PQ} \\ H_{QP} & H_{QQ} \end{pmatrix} \begin{pmatrix} P\Psi \\ Q\Psi \end{pmatrix} = E\,T \begin{pmatrix} P\Psi \\ Q\Psi \end{pmatrix} \tag{10}$$

where $H_{PP} = PHP$, $H_{QP} = QHP$, etc.

Multiplying the matrices in (10) leads to:

$$H_{PP}P\Psi + H_{PQ}Q\Psi = EP\Psi \tag{11}$$

and

$$H_{QP}P\Psi + H_{QQ}Q\Psi = EQ\Psi. \tag{12}$$

From Eq.(12) we have,

$$Q\Psi = H_{QP}P\Psi/(E - H_{QQ}). \tag{13}$$

Substituting Eq.(13) into Eq.(11) leads to a matrix optical potential for $P\Psi$,

$$(H_{PP} + H_{PQ}H_{QP}/(E - H_{QQ}))\ P\Psi = EP\Psi. \tag{14}$$

It is difficult to solve (14) directly for $P\Psi$ since E is on both sides of the equation. Nevertheless, $P\Psi$ can be determined by retaining the coefficients of the $P\Psi$ terms resulting from the diagonalization of the H matrix in Eq.(10). Before diagonalizing H we must project out the low energy $Q\Psi$ roots in order to prevent them from mixing into $P\Psi$. Therefore, it is necessary to first solve for the $Q\Psi$ roots by diagonalizing H_{QQ}. The H_{QQ} portion of the H matrix in Eq.(10) is transformed to project out the physically meaningful $Q\Psi$ roots. $P\Psi$ is then determined by diagonalizing the new H matrix with the transformed H_{QQ}. The net effect is to provide additional correlation to the $P\Psi$ space from the nonphysical roots in the Q space. $P\Psi$'s for successive principal quantum numbers are used to represent Ψ_I^C in Eq.(4). The widths obtained by this procedure are then extrapolated to the continuum as described above. The importance of the correlation added to the P space from the higher terms in Q space has been emphasized by Hazi who has described an approach similar to that used here.[23]

An application of this approach to the calculation of the widths of the B and L $^2\Pi$ states of NO has already been discussed.[24] An additional example of this approach is given in Table 1. for the O_2 $^3\Pi_g$ width. This is the only O_2 width for which there are experimentally derived matrix elements for comparison. An analysis of the released kinetic energy line width for the v=1 level of the $C^3\Pi_g$ state of O_2 indicates that the electronic matrix element between the C Rydberg state and the lowest valence $^3\Pi_g$ state is 0.079eV.[8] An additional determination based on the experimental line widths of the lowest 4 vibrational levels of the C state obtains a matrix element of 0.0625(+0.006,-0.004)eV.[9]

All calculations in Table 1. have been done at $R=2.2819a_o$. A [3s,2p,1d] basis set on each center was supplemented with a set a 18 diffuse s Gaussians at the midpoint and the Rydberg orbitals were determined by the Improved Virtual Orbital method.[25] The $^3\Pi_g$ valence state was described with a full valence CI consisting of 46 terms. For the C state, a valence CI on the ion ground state was coupled with the Rydberg orbital and each of the three valence virtual σ_g orbitals leading to a 636 term CI. Using the procedure outlined above leads to

the widths shown in Table 1. Using the widths for n=8,9 gives the expression, $\Gamma = 0.00217\exp(1.39/n^{*}-(0.5/n^{*2}))$. The extrapolated width for $n^{*}\rightarrow\infty$ is 0.00217eV. This width is about two orders of magnitude smaller than the widths for the three important dissociative routes identified above. As a result, the $^{3}\Pi_{g}$ state was not included in the DR rate coefficient calculations discussed below.

Table 1. Electron-Ion Capture Widths (Γ) from $^{3}\Pi_{g}$ Rydberg States

n	n*	$\rho(eV^{-1})$	Γ(eV)
9	7.8897	17.903	0.00257
8	6.8896	11.892	0.00263
7	5.8902	7.4022	0.00272
6	4.8913	4.2110	0.00285
5	3.8930	2.0972	0.00311
4	2.8959	0.84005	0.00367
3	1.8984	0.21774	0.00522

The matrix element calculated here for n=3 is 0.0617eV. Since the electronic matrix element varies with R, the experimentally derived matrix element is an averaged value. However, since the variation of the matrix element with R over the relevant range of nuclear vibrations is estimated to be less than about 10%, the results show that relatively small wave functions can yield interaction matrix elements that are in good agreement with experiment.

5. DR RATE COEFFICIENTS FOR O_2

The expression for the direct DR cross section derived by Giusti[26] has been used to calculate cross sections and rate coefficients for generation of $O(^{1}S)$ and $O(^{1}D)$ along the $^{1}\Sigma_{u}^{+}$, $B^{3}\Sigma_{u}^{-}$, and $^{1}\Delta_{u}$ diabatic potential curves described above. For DR leading to $O(^{1}S)$,[18] the v=2 level of the ion has the highest rate coefficient for the lowest eight vibrational levels and is a factor of 78 greater than the coefficient from v=0 at an electron temperature (T_{e}) of 300K. A comparison of the calculated rate coefficients to those deduced from atmospheric models shows that the atmospheric models apply to molecular ions which are not

in a Boltzmann distribution but which are instead significantly populated in the v>0 levels. In contrast to the situation for $O(^1S)$ generation, the total rate coefficient[19] for producing $O(^1D)$ is greatest from v=0 and is a factor of 1.9 greater than the coefficient from v=2 at T_e=300K. The rate coefficient for v=0 is in good agreement with those deduced from atmospheric models. The calculations show that the dominant route for producing $O(^1D)$ from v=0 is $^1\Delta_u$ and $^3\Sigma_u^-$ is the dominant route from v=1 and v=2.

Table 2. DR Rate Coefficients for Production of $O(^1S)$ for $600 \leq T_e \leq 1000$K.

Ion Vibrational Level	Rate Coefficient(cm^3/sec)[a]
0	0.24(+.12,-.08)[-0.14]
1	5.0(+1.2,-1.1)[-0.36]
2	15.(+2.,-3.)[-0.50]
3	4.8(+3.3,-2.3)[-0.77]
4	4.9(+0.6,-1.2)[-0.32]
5	1.2(+1.9,-0.9)[-0.90]
6	5.1(+0.6,-1.1)[-0.56]
7	1.4(+0.9,-0.9)[+0.06]

a. All rate coefficients have been multiplied by 10^9. The exponent of the temperature dependence is in square brackets. The rate coefficient for v=0 is $2.4(+1.2,-0.8)\times10^{-10}\times((T_e/800)^{-0.14})cm^3$/sec.

Since the electron temperatures in ionospheric models are near 800K, we list in Table 2. the rate coefficients for producing $O(^1S)$ for $600 \leq T_e \leq 1000$K for each of the lowest eight ion vibrational levels.

Table 3. DR Rate Coefficients for Production of $O(^1D)$ for $600 \leq T_e \leq 1000$K.

Ion Vibrational Level	Rate Coefficient(cm^3/sec)[a]
0	1.37(+.14,-.16)[-0.51]
1	1.09(+.12,-.14)[-0.55]
2	0.78(+.13,-.16)[-0.41]

a. All rate coefficients have been multiplied by 10^7. The exponent of the temperature dependence is in square brackets. The rate coefficient for v=0 is $1.37(+.14,-.16)\times10^{-7}\times((T_e/800)^{-0.51})cm^3$/sec.

Because of the position of the intersection of the dissociative curve with the v=5 level, the coefficient from v=5 is highly sensitive to an energetic displacement of the dissociative route within its expected uncertainty (0.1eV). Table 3 has the $O(^1D)$ rate coefficients in the

same temperature range from each of the lowest three ion vibrational levels.

6. DISSOCIATIVE ROUTES FOR N_2

Preliminary results are reported here which identify the important dissociative routes for the v=0 level of the ground state of N_2^+. These results are based on large scale second order CI calculations using atomic natural orbital basis sets.[27] The details will be reported separately.

The dominant dissociative routes from v=0, $2^1\Sigma_g^+(^2D + {}^2D)$, $C'^3\Pi_u(^4S + {}^2P)$, $3^3\Pi_u(^2D + {}^2D)$, and $G^3\Delta_g(^4S + {}^2D)$, are shown in Fig. 2.

The dominant configuration of the $2^1\Sigma_g^+$ state is

$$....(3\sigma_g)^2(1\pi_{ux})\ (1\pi_{uy})\ (1\pi_{gx})\ (1\pi_{gy})$$

where .... denotes $(1\sigma_g)^2(1\sigma_u)^2(2\sigma_g)^2(2\sigma_u)^2$. This configuration differs by a triple excitation from the dominant configuration of the ion plus a "free" or Rydberg electron,

$$....(3\sigma_g)\ (1\pi_{ux})^2(1\pi_{uy})^2(RYD\sigma_g).$$

The matrix element of the Hamiltonian between these two configurations is zero and these dominant terms will not contribute to the electron capture width. The magnitude of the width will be determined by matrix elements between secondary terms in both states and may be small. As a result, $2^2\Sigma_g^+$ may make only a small contribution to the total DR rate coefficient from v=0.

The G state also passes through the v=0 level of the ion and dissociates to $^4S + {}^2D$ giving atoms with 1.72eV kinetic energy from v=0. The dominant configurations of this state,

$$....(3\sigma_g)^2(1\pi_{ux})\ (1\pi_{uy})\ (1\pi_{gx})^2,$$
$$....(3\sigma_g)^2(1\pi_{ux})\ (1\pi_{uy})\ (1\pi_{gy})^2,$$
$$....(3\sigma_g)^2(1\pi_{ux})^2(1\pi_{gx})\ (1\pi_{gy}),$$
$$....(3\sigma_g)^2(1\pi_{gx})^2(1\pi_{gx})\ (1\pi_{gy}),$$

differ from the ion plus a continuum electron by a triple excitation. Therefore, as for $2^2\Sigma_g^+$, the dominant configurations will not contribute

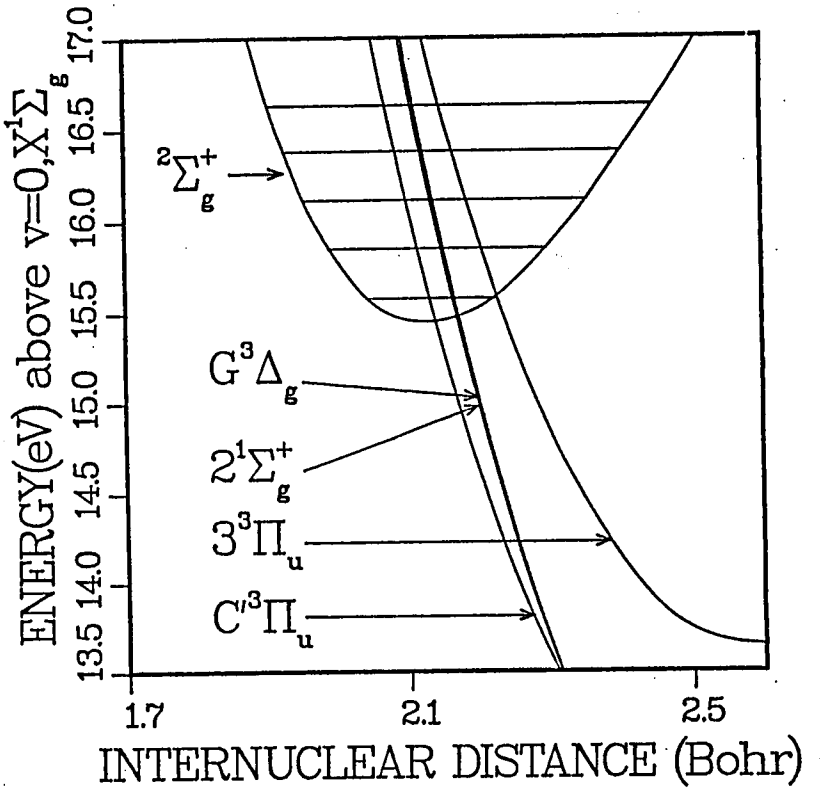

Fig. 2 Dissociative routes for the v=0 level of N_2^+. The ion potential is from Ref. 14.

to the width and this state is likely to have a small width and a small DR rate coefficient. This is an important conclusion for the escape of N atoms from Mars since this state and possibly the C' state (through an avoided crossing with the C state) are the only states that can supply enough kinetic energy for escape from v=0.

The primary configuration of the C' and $3^3\Pi_u$ states,

$$....(3\sigma_g)\ (1\pi_{ux})^2(1\pi_{uy})\ (1\pi_{gx})\ (1\pi_{gy}),$$

differs by a double excitation from the ion ground state plus a continuum electron. The capture width for this state may be larger than that for $2^1\Sigma_g^+$ and $G^3\Delta_g$ and it appears that these $^3\Pi_u$ states may be the dominant states for DR from v=0. The importance of the $^3\Pi_u$ states is in

good agreement with the results of Michels.[28] The C' state has an avoided crossing with the lower $C^3\Pi_u$ state which dissociates to $^4S + ^2D$ atoms. The determination of the states of the product atoms due to initial dissociation along the C' state is currently under study.

7. THE ROLE OF RYDBERG STATES IN DIRECT DR OF N_2^+

Rydberg state potential curves having the ground state of the ion as core cannot cross the ground state of the ion and in addition have very small electron capture widths. These states are usually not important for direct DR electron capture. However, because the first excited state of N_2^+ is only 1.1eV above the ground state, Rydberg states having the excited state core can cross the ground state of the ion and provide routes for DR.

For $^1\Sigma_g^+$ symmetry, an N_2 Rydberg state can be formed by binding a π_u Rydberg orbital to the excited $A^2\Pi_u$ state of N_2^+. This state will have an avoided crossing with the $2^1\Sigma_g^+$ state described above and can provide a channel for DR. A comparison to analogous states in O_2 indicates that the $4p\pi$ $^1\Sigma_g^+$ state having the A core will pass through the ground state of N_2^+ near the equilibrium separation. If the $4p\pi$ $^1\Sigma_g^+$ state should prove to have a large capture width, this route could be an important route for DR in N_2^+. The calculation of the potential curve for this state and the electron capture width are in progress. While the Rydberg states are diffuse, their primary configurations differ from the ion by a double excitation and they may have larger electronic widths than the $^1\Sigma_g^+$ valence state which has primary terms that differ from the ion plus a continuum electron by a triple excitation. It appears that a multistate treatment involving both the valence states and the excited core Rydberg states may be needed to calculate the cross sections for DR of N_2^+.

8. ACKNOWLEDGEMENT

This research was supported by the National Science Foundation under grant ATM-8616776 and by the National Center for Atmospheric Research

which is sponsored by the National Science Foundation. Support was also provided by NASA Grant NAGW-1404, by the Air Force Office of Scientific Research under grant AFOSR-84-0109 and by NASA Cooperative Agreement NCC 2-308.

9. REFERENCES

1. J. Kaplan, Phys. Rev. 38, 1048(1931).

2. D. R. Bates and H. S. W. Massey, Proc. Roy. Soc.(Lond.)192, 1(1947).

3. J. L. Queffelec, B. R. Rowe, M. Morlais, J. C. Gomet, and F. Vallee, Planet. Space Sci. 33, 263(1985).

4. D. Kley, G. M. Lawrence, and E. C. Stone, J. Chem. Phys. 66, 4157(1977).

5. E. C. Zipf, Planet. Space Sci. 36, 621(1988).

6. R. Galluser and K. Dressler, J. Chem. Phys. 76, 4311(1982); M. Raoult, J. Chem. Phys. 87, 4736(1987).

7. H. Lefebvre-Brion, Can. J. Phys. 47, 541(1969); D. Stahel, M. Leoni, and K. Dressler, J. Chem. Phys. 79, 2541 (1983).

8. W. J. van der Zande, W. Koot, J. Los, and J. R. Peterson, Predissociation of 3s $^{1,3}\Pi_g$ and $^{3,5}\Pi_u$ Rydberg States of O_2: Mechanisms and Pathways, this volume.

9. R. Friedman, private communication.

10. S. Huzinaga, J. Chem. Phys. 42, 1293(1965).

11. T. H. Dunning, Jr., J. Chem. Phys. 55, 716(1971).

12. P. Siegbahn, A. Heiberg, B. Roos, and B. Levy, Phys. Scr. 21, 323 (1980); P. E. M. Siegbahn, J. Almhof, A. Heiberg, and B.O. Roos, J. Chem. Phys. 74, 2384 (1981).

13. P. E. M. Siegbahn, J. Chem. Phys. 72, 1647(1980).

14. A. Lofthus and P. H. Krupenie, J. Phys. Chem. Ref. Data 6, 113(1977).

15. P. H. Krupenie, J. Phys. Chem. Ref. Data,1, 423(1972).

16. A. C. Allison, S. L. Guberman, and A. Dalgarno, J. Geophys. Res. in press,(1986).

17. S. L. Guberman, Potential Energy Curves for Dissociative Recombination, in Physics of Ion-Ion and Electron-Ion Collisions ed. by F. Brouillard (Plenum, New York, 1983) pp. 167-200.

18. S. L. Guberman, Nature 327, 408 (1987).

19. S. L. Guberman, Planet. Space Sci. 36, 47 (1988).

20. M. J. Seaton, Rep. Prog. Phys. 46, 167(1983).

21. H. Feshbach, Ann. Phys. (N. Y.) 5, 357(1958).

22. P. O. Lowdin, in Perturbation Theory and Its Application in Quantum Mechanics, ed. by C. H. Wilcox (John Wiley and Sons, N. Y., 1966), p.255; P. O. Lowdin, Advan. Chem. Phys. 2, 207 (1959); P. O. Lowdin, J. Math. Phys. 3, 969 (1962).

23. A. U. Hazi, Molecular Resonance Phenomena, in Electron-Atom and Electron-Molecule Collisions, ed. by J. Hinze,(Plenum Press, New York, 1983), p.103.

24. S. L. Guberman, Theoretical Studies of Dissociative Recombination, in Thermophysical Aspects of Re-entry Flows, ed. by J. N. Moss and C. D. Scott, (American Institute of Aeronautics and Astronautics, New York, 1986) pp.225-242.

25. W. J. Hunt and W. A. Goddard III, Chem. Phys. Lett. 6, 414(1969).

26. A. Giusti, J. Phys. B 13, 3867 (1980).

27. J. Almlof and P. R. Taylor, J. Chem. Phys. 86, 4070 (1987).

28. H. H. Michels, Electronic Structure of Excited States of Selected Atmospheric Systems, in The Excited State in Chemical Physics, ed. by J. M. McGowan (Wiley, New York, 1981), Vol 2; H. H. Michels, Abstracts of the Third Int. Conference on Atomic Physics, 173 (1972).